

FUZZY DETECTORS AGAINST ADVERSARIAL ATTACKS

Yi Li, Plamen Angelov, Neeraj Suri

School of Computing and Communications, Lancaster University, UK

ABSTRACT

Deep learning-based methods have proved useful for adversarial attack detection. However, conventional detection algorithms exploit crisp set theory for classification boundary. Therefore, representing vague concepts is not available. Motivated by the recent success in fuzzy systems, we propose a fuzzy rule-based neural network to improve adversarial attack detection accuracy. The pre-trained ImageNet model is exploited to extract feature maps from clean and attacked images. Subsequently, the fuzzification network is used to obtain feature maps to produce fuzzy sets of difference degrees between clean and attacked images. The fuzzy rules control the intelligence that determines the detection boundaries. In the defuzzification layer, the fuzzy prediction from the intelligence is mapped back into the crisp model predictions for images. The loss between the prediction and label controls the rules to train the fuzzy detector. We show that the fuzzy rule-based network learns rich feature information than binary outputs and offers to obtain an overall performance gain. Our experiments, conducted over a wide range of images, show that the proposed method consistently performs better than conventional crisp set training in adversarial attack detection with various fuzzy system-based neural networks. The source code of the proposed method is available at <https://github.com/Yukino-3/Fuzzy>.

Index Terms— Deep learning, adversarial attack detection, classification boundary, fuzzy rule, fuzzy prediction

1. INTRODUCTION

Adversarial attack detection, aiming to defend applications by detecting attacks using the difference between adversarial and clean image samples, is an important security topic useful in many real-world applications such as autonomous driving systems, object detection, medical image processing, and robotics [1]. Recently, a variety of deep learning approaches have been proposed [2], for adversarial attack detection mainly divided into empirical statistics-based detection [3], image pre-processing and reconstruction-based detection [4], and detection networks [5]. In this paper, we focus on image pre-processing and reconstruction-based detection by using deep learning techniques.

A neural network typically predicts a *crisp* result, namely,

a value 1 when the sample is attacked and 0 when it is clean. The loss between the crisp prediction and crisp label is then exploited to train the model. While some recent studies have explored the fuzzy classifier in adversarial attack detection [6, 7], crisp set-based detection methods [4, 8, 9] are the common choices as the crisp sets can easily be estimated from the input data. The crisp set-based detection methods directly determine whether an image is clean or attacked. However, calculating the loss is non-differentiable and hinders training through normal back-propagation.

In recent studies, the fuzzy system is shown to offer several advantages in handling crisp set-based problems. It allows representation imprecision of objects, relations, and knowledge, and aims at different levels of latent representation [10, 11]. It constitutes a unified framework for representing and processing both numerical and symbolic information, as well as structural information (constituted mainly by spatial relations in image processing) [12]. Hence this theory can potentially handle tasks at several levels, from a low level (e.g., binary classification) to a high level (e.g., model-based structural recognition and scene interpretation). It provides a flexible framework for information fusion as well as powerful tool support for reasoning and decision-making [13]. In this paper, we show how the use of fuzzy detectors offers significant benefits in adversarial attack detection. Specifically, we propose a fuzzification process with fuzzy rules of difference degree between clean and attacked images.

2. PROPOSED APPROACH FOR FUZZY DETECTORS

Fig. 1 illustrates the architectural approach of our proposed fuzzy detector. Conceptually, the feature maps from the attacked and clean images \mathcal{F}_a and \mathcal{F}_c constitute the inputs of the proposed fuzzy detector. The loss between the feature maps is converted into the fuzzy set for the intelligence (I).

The input of the encoder is either clean or attacked images with hard labels, i.e., clean or attacked. The attacked images are constructed with random error rates from 0.01 to 0.04 as in contemporary works. The ImageNet pre-trained model obtains these images and extracts their feature maps. The feature maps of clean and attacked images are presented as \mathcal{F}_c and \mathcal{F}_a , respectively. The proposed fuzzy system-based detector then aims to map from the feature space to the label space. To

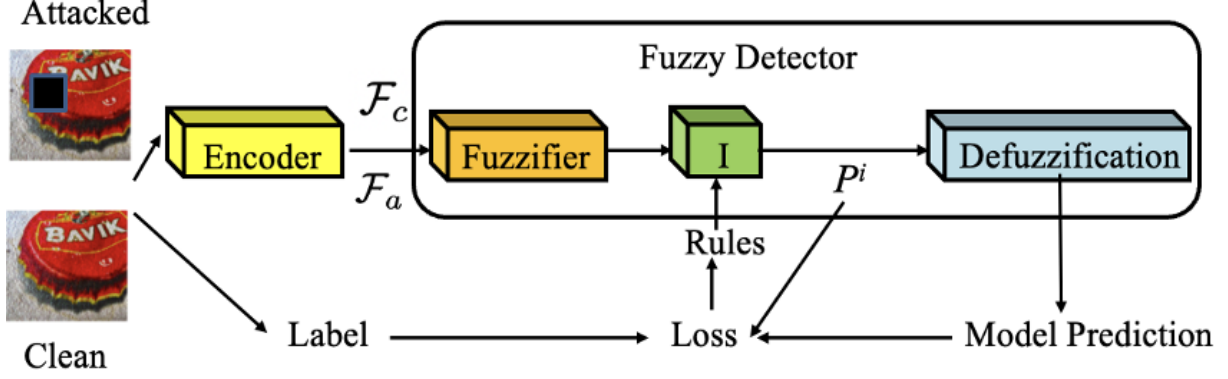


Fig. 1. The architecture of the proposed fuzzy detector.

achieve that, we propose a fuzzy detector with its constituent blocks progressively detailed in the following sections.

2.1. Fuzzifier

As aforementioned, the loss between \mathcal{F}_c and \mathcal{F}_a is required to be calculated. Subsequently, the fuzzifier converts the loss into a fuzzy set to describe the difference degrees between feature maps at the pixel level. The degree of differences in the fuzzy set quantifies the difference levels across the feature maps of clean and attacked images. The membership function μ is illustrated in Fig. 2.

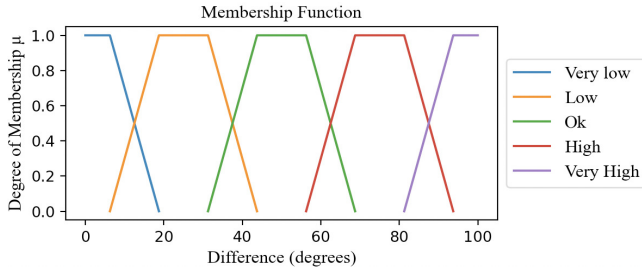


Fig. 2. The membership function.

2.2. Fuzzy Rules

Intelligence is controlled by rules that determine the detection boundaries. The rules of the proposed fuzzifier follow commonly used fuzzy-rule-based classifiers [10, 11] as:

$$R^i : \text{IF } (x_1 \text{ is around } x_1^{i*}) \text{ AND } (x_2 \text{ is around } x_2^{i*}) \\ \text{AND} \dots \dots \text{AND } (x_n \text{ is around } x_n^{i*}) \text{ THEN } (P^i) \quad (1)$$

where $x = [x_1, x_2, \dots, x_n]^T$ is the pixels of feature maps. In the intelligence layer, $(x_j \text{ is around } x_j^{i*})$ indicates the j th fuzzy set of the i th fuzzy rule R^i . To achieve that, we consider the Euclidian Distance d between x_j and x_j^{i*} with a

hyperparameter α_j . When the distance d is smaller than α_j , the fuzzy prediction with the i th fuzzy rule is P^i that predicts how much the model trusts the image. The hyperparameter α_j is further updated to improve the boundary accuracy in the training stage.

2.3. Defuzzification

A centroid defuzzification method is exploited to convert the fuzzy prediction set into the model prediction [14]. Particularly, the center of gravity of the fuzzy set is calculated along the difference degree as:

$$P = \frac{\sum_i \mu(P_i) P_i}{\sum_i \mu(P_i)} \quad (2)$$

where P is the model prediction, i.e., 0 or 1 for clean or attacked image, respectively.

2.4. Training

The training loss is calculated as follows. Firstly, we calculate the fuzzy loss $\mathcal{L}_{\mathcal{F}}$ between the label and fuzzy prediction. Secondly, the overall loss \mathcal{L} is calculated by the loss between the label and model prediction $\mathcal{L}_{\mathcal{M}}$ with hyperparameters λ_1 and λ_2 as:

$$\mathcal{L} = \begin{cases} \lambda_1 \cdot \mathcal{L}_{\mathcal{F}}, & \text{if } \mathcal{L}_{\mathcal{M}} \neq 0 \\ \mathcal{L}_{\mathcal{F}} / \lambda_2, & \text{otherwise} \end{cases} \quad (3)$$

Both λ_1 and λ_2 are empirically set between 1 and 10 over the different experiments. The fuzzy rules are refined by \mathcal{L} and control the intelligence that makes more accurate fuzzy predictions. The pseudo-code of the proposed fuzzy rule-based attack detection method is summarized in Algorithm 1.

3. EXPERIMENTAL RESULTS

3.1. Datasets

We perform experiments on several public datasets, including ImageNet-R [16], Canadian Institute For Advanced Research-

Algorithm 1: Fuzzy rule-based detector.

Input: Feature maps \mathcal{F}_c and \mathcal{F}_a , Label X , learning rate η , epoch E_{\max} ,

Output: Model prediction P

Data: Training set \mathcal{D}

```
1 Initialize  $R^i, \mu$ ;  
2 Initialize hyperparameters  $\lambda_1, \lambda_2, \alpha_j$  and  $\theta$ ;  
3 for  $E = 1, 2, \dots, E_{\max}$  do  
4    $\mathcal{L}_{\mathcal{F}} = H(\mathcal{F}_c, \mathcal{F}_a)$  // Calculate the cross entropy  
   loss;  
5   if  $d(x_j, x_j^{i*}) < \alpha_j$  then  
6      $P_i = \theta(\mathcal{F}_a)$ ;  
7   end  
8    $P \leftarrow P_i, \mu$  // Defuzzification;  
9   if  $X = P$  then  
10     $\mathcal{L} = \mathcal{L}_{\mathcal{F}}/\lambda_2$ ;  
11  else  
12     $\mathcal{L} = \lambda_1 \cdot \mathcal{L}_{\mathcal{F}}$   
13  end  
14   $\theta, \mu \leftarrow \mathcal{L}_{\mathcal{F}}$ ;  
15   $\lambda_1, \lambda_2 \leftarrow \mathcal{L}$  // Update hyperparameters ;  
16 end
```

10 (CIFAR-10) [17], Common Object and Concept (COCO) [18], and ImageNet Large Scale Visual Recognition Challenge (ILSVRC) [19]. We randomly select 50,000, 10,000, and 10,000 images from each dataset for the training, validation, and test stages.

3.2. Attacks and Performance Measure

The adversarial samples from these datasets are constructed using the Fast Gradient Sign Method (FGSM) [20], Projected Gradient Descent (PGD) [21], and Semantic similarity attack on high-frequency components (SSAH) [22] attacks. We select these attacks because they are robust to novel adversarial attack detection and defense techniques [22, 15]. The error rate is randomly set from 0.01 to 0.04 for training and test data similar to as in contemporary works [15, 4].

In the experiment, the detection rate (DR) [15] is used as the performance measure.

$$DR(\%) = \frac{TP + TN}{TP + TN + FP + FN} \times 100 \quad (4)$$

where TP and TN are true positive and true negative results, and FP and FN are false positive and false negative results. Moreover, we evaluate the true positive on clean image samples as:

$$DR(\%) = \frac{TP}{TP + TN} \times 100 \quad (5)$$

3.3. Model Configuration

The pre-trained EfficientNetV2-XL [23] on the ILSVRC dataset is exploited to extract features. We select this model because it achieves the state-of-the-art benchmark on the ILSVRC challenge. Moreover, we apply the proposed fuzzy detector on different backbones, e.g., Res2Net-v1b-101 [24], YOLOX-L [25], and PRB-FPN6-2PY [26]. Different from the pre-trained encoder, these models are initialized and re-trained with fuzzy logic.

At training stage, the proposed model is trained using the M-SGD optimizer with a learning rate set empirically to 0.0008 according to a grid search. The batch size is set to 32. We train the networks for 200 epochs. All experiments are run on the High End Computing (HEC) Cluster with Tesla V100 GPUs.

3.4. Results

3.4.1. Comparison with Same Attacks

In the first experiment, we compare the proposed method to state-of-the-art adversarial attack detection methods [1, 15, 6, 8, 9] with the same attack between the training and test stage. The proposed fuzzy detector-based Res2Net-v1b-101, YOLOX-L, and PRB-FPN6-2PY are simplified as F-Res, F-YL, and F-PF, respectively.

From Tables I & II, it can be observed that: (1) In all the evaluated models, the proposed methods with different backbones offer the best effectiveness. Different from crisp set-based decision-making pipelines, the proposed fuzzy detectors convert the loss between feature maps into fuzzy sets and provide difference scores ('high', 'ok', and 'low'). Therefore, the proposed method exploits more feature information than binary decisions. The fuzzy rules are trained with difference scores to help the detector make more accurate decisions. (2) The proposed F-YL model offers the best attack detection performance on all datasets. The reason is likely due to the combined implicit knowledge and explicit knowledge in the YOLOX decoder [25]. (3) Compared to the improvement in FGSM, PGD, and SSAH attacks, the improvement of detection accuracy tends to fall drastically when evaluating the true positives on clean image samples. For example, compared to ESMAF model, the proposed F-YL obtain 7.9% improvement on PGD attacked CIFAR-10 dataset, while it is only 2.8% on the true positive evaluation.

3.4.2. Comparison with Different Attacks

In this experiment, we compare the proposed method to state-of-the-art adversarial attack detection methods [1, 15, 6, 8, 9] with different attacks between the training and test stage. To achieve that, we randomly select an unseen attack to construct the test data in Tables III & IV.

Table 1. Attack detection ratio on the CIFAR-10 and ImageNet-R datasets. Each result is the average of 10,000 experiments. **Bold** indicates the best results. *Italic* shows the proposed methods.

Method	Detection Ratio (%)							
	CIFAR-10				ImageNet-R (%)			
	Clean	FGSM	PGD	SSAH	Clean	FGSM	PGD	SSAH
FCB [6]	75.5 ± 1.8	49.8 ± 1.5	47.1 ± 1.0	43.6 ± 1.8	75.2 ± 1.9	48.5 ± 1.8	46.8 ± 1.9	43.9 ± 1.4
SAC [1]	78.7 ± 1.5	60.1 ± 2.3	59.7 ± 2.2	56.8 ± 2.4	78.0 ± 1.9	58.9 ± 2.0	57.5 ± 2.1	52.9 ± 1.8
sim-DNN [15]	81.8 ± 1.0	70.5 ± 1.4	60.0 ± 1.6	49.4 ± 0.7	80.9 ± 1.5	71.0 ± 1.7	66.2 ± 1.3	61.4 ± 1.1
DTBA [8]	85.7 ± 1.3	78.3 ± 1.2	75.6 ± 1.0	71.7 ± 0.8	85.2 ± 1.0	78.0 ± 1.1	72.4 ± 1.1	68.9 ± 0.8
ESMAF [9]	87.4 ± 1.0	80.5 ± 1.6	76.9 ± 1.9	75.4 ± 0.7	87.4 ± 1.2	79.7 ± 1.3	75.6 ± 0.9	71.8 ± 0.6
<i>F-Res</i>	89.1 ± 0.5	86.3 ± 1.0	83.5 ± 0.7	82.1 ± 0.9	89.0 ± 0.5	86.0 ± 1.1	82.8 ± 1.2	80.2 ± 0.8
<i>F-PF</i>	89.9 ± 0.8	86.5 ± 0.7	82.3 ± 1.2	80.8 ± 0.8	89.9 ± 0.8	87.0 ± 1.3	81.6 ± 1.0	80.8 ± 0.9
<i>F-YL</i>	90.2 ± 0.4	87.2 ± 0.5	84.8 ± 0.9	84.1 ± 0.4	89.9 ± 0.7	87.0 ± 1.2	83.4 ± 0.7	82.9 ± 0.5

Table 2. Attack detection ratio on the COCO and ILSVRC datasets. Each result is the average of 10,000 experiments. **Bold** indicates the best results. *Italic* shows the proposed methods.

Method	Detection Ratio (%)							
	COCO				ILSVRC (%)			
	Clean	FGSM	PGD	SSAH	Clean	FGSM	PGD	SSAH
FCB [6]	72.7 ± 1.6	47.2 ± 1.6	46.5 ± 1.9	40.6 ± 2.0	76.8 ± 1.5	51.2 ± 2.2	50.4 ± 1.5	48.5 ± 2.5
SAC [1]	78.0 ± 2.0	49.6 ± 2.1	48.4 ± 2.0	45.9 ± 1.9	80.2 ± 2.2	63.6 ± 1.6	63.0 ± 2.0	59.4 ± 1.9
sim-DNN [15]	79.3 ± 2.0	66.8 ± 2.0	64.3 ± 2.2	60.0 ± 1.8	82.5 ± 1.3	75.2 ± 2.1	72.5 ± 1.6	69.6 ± 1.5
DTBA [8]	83.1 ± 0.9	75.3 ± 1.1	71.0 ± 1.4	68.7 ± 1.0	86.8 ± 0.7	81.1 ± 1.4	80.5 ± 0.8	76.0 ± 0.9
ESMAF [9]	85.0 ± 1.1	76.5 ± 1.3	74.2 ± 1.6	70.8 ± 1.0	87.9 ± 1.0	82.6 ± 2.0	77.0 ± 2.1	75.2 ± 0.9
<i>F-Res</i>	88.4 ± 0.6	84.0 ± 1.4	80.7 ± 1.5	78.6 ± 1.2	89.7 ± 0.8	86.9 ± 1.2	84.1 ± 0.6	82.8 ± 1.1
<i>F-PF</i>	89.8 ± 0.3	85.8 ± 1.2	82.0 ± 1.0	80.1 ± 1.1	90.3 ± 0.4	87.3 ± 1.0	82.4 ± 1.1	81.2 ± 0.6
<i>F-YL</i>	89.8 ± 0.3	86.8 ± 0.9	84.0 ± 1.1	84.1 ± 0.8	91.0 ± 0.3	87.9 ± 0.7	85.9 ± 0.9	84.4 ± 0.8

Table 3. Attack detection ratio on the CIFAR-10 and ImageNet-R datasets with unseen attacks. Each result is the average of 10,000 experiments. **bold** indicates the best results. *Italic* shows the proposed methods.

Method	Detection Ratio (%)							
	CIFAR-10				ImageNet-R (%)			
	Clean	FGSM	PGD	SSAH	Clean	FGSM	PGD	SSAH
FCB [6]	73.6 ± 1.9	46.3 ± 1.4	45.2 ± 1.3	40.7 ± 2.0	72.0 ± 2.1	44.9 ± 1.9	44.5 ± 1.9	41.4 ± 1.7
SAC [1]	74.8 ± 1.6	57.7 ± 2.2	56.0 ± 2.5	53.5 ± 2.6	74.9 ± 2.1	56.0 ± 2.3	53.9 ± 2.4	50.2 ± 2.0
sim-DNN [15]	79.5 ± 1.2	67.9 ± 1.6	56.9 ± 1.8	47.5 ± 1.0	77.6 ± 1.8	68.8 ± 1.6	65.1 ± 1.5	60.1 ± 1.2
DTBA [8]	84.2 ± 1.6	77.0 ± 1.4	74.0 ± 1.1	70.2 ± 1.1	83.9 ± 1.4	76.4 ± 1.3	70.9 ± 1.2	67.3 ± 1.2
ESMAF [9]	84.8 ± 1.3	77.9 ± 1.5	74.3 ± 2.2	73.8 ± 0.9	84.7 ± 1.5	77.1 ± 1.6	72.9 ± 1.2	70.0 ± 1.0
<i>F-Res</i>	88.8 ± 0.5	85.9 ± 0.9	82.8 ± 0.9	81.6 ± 1.1	88.5 ± 0.7	85.7 ± 1.5	82.7 ± 1.1	79.4 ± 0.9
<i>F-PF</i>	89.8 ± 0.6	86.3 ± 0.6	82.0 ± 1.2	80.4 ± 0.9	89.5 ± 0.9	86.8 ± 1.1	81.4 ± 1.1	80.7 ± 1.0
<i>F-YL</i>	89.4 ± 0.6	86.4 ± 0.7	83.6 ± 1.0	82.8 ± 0.7	89.0 ± 0.4	85.9 ± 1.5	82.0 ± 0.8	82.6 ± 0.5

Table 4. Attack detection ratio on the COCO and ILSVRC datasets with unseen attacks. Each result is the average of 10,000 experiments. **Bold** indicates the best results. *Italic* shows the proposed methods.

Method	Detection Ratio (%)							
	COCO				ILSVRC (%)			
	Clean	FGSM	PGD	SSAH	Clean	FGSM	PGD	SSAH
FCB [6]	69.9 ± 1.7	45.8 ± 1.7	44.8 ± 2.2	38.9 ± 2.4	74.0 ± 1.7	48.4 ± 2.0	47.8 ± 1.8	45.9 ± 2.8
SAC [1]	72.8 ± 2.1	48.2 ± 2.1	45.9 ± 2.2	44.5 ± 2.1	78.7 ± 2.3	60.8 ± 1.4	61.7 ± 2.1	57.6 ± 2.2
sim-DNN [15]	78.8 ± 2.4	63.6 ± 1.9	62.5 ± 2.0	57.8 ± 2.1	82.0 ± 1.6	74.3 ± 2.4	70.3 ± 1.9	66.8 ± 1.8
DTBA [8]	82.4 ± 1.1	74.6 ± 1.6	70.1 ± 1.8	67.6 ± 1.5	86.3 ± 0.5	79.7 ± 1.8	79.0 ± 1.2	74.7 ± 1.5
ESMAF [9]	82.2 ± 1.1	72.9 ± 1.9	72.0 ± 2.0	67.1 ± 1.8	84.3 ± 1.9	80.2 ± 2.2	73.8 ± 2.5	72.9 ± 1.6
<i>F-Res</i>	88.3 ± 0.5	83.3 ± 1.4	80.1 ± 1.9	77.9 ± 1.4	89.5 ± 1.0	86.0 ± 1.3	83.3 ± 0.8	81.7 ± 1.5
<i>F-PF</i>	89.7 ± 0.4	85.2 ± 1.1	81.6 ± 1.4	79.8 ± 1.2	89.9 ± 0.6	87.0 ± 0.9	82.1 ± 1.4	80.8 ± 0.8
<i>F-YL</i>	89.0 ± 0.6	85.6 ± 1.2	82.9 ± 1.2	82.8 ± 1.0	90.0 ± 0.5	86.8 ± 1.0	85.0 ± 0.8	83.1 ± 1.3

From Tables III & IV, it can be observed that in all the evaluated models, the proposed fuzzy rule-based methods with different backbones offer the best effectiveness. The goal of the adversarial training provided by the DTBA and DSMAF is to increase the model’s robustness, however, they lack generalisation to unseen domains, i.e., datasets and attacks. The proposed fuzzy detector maintains its performance stable even when adversarial or clean images from unknown datasets are presented to the detection model due to its inner fuzzy rules and detection mechanism that was projected for such scenarios.

The visualizations are shown in Fig. 3 as related to the reconstructions after detecting attacks of three randomly selected images from the COCO dataset. After comparing the reconstructed images with the original and attacked images, it can be observed that the reconstructions obtained via the proposed method, i.e., Fig. 3 (d), are closer to original images, which again confirms the efficacy of the proposed method.

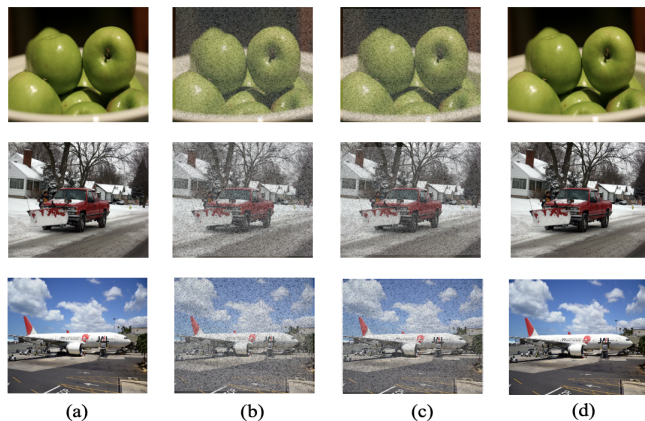


Fig. 3. Attack detection results: (a) original images; (b)&(c) attacked by random attack types and error rates; (d) reconstruction from attacks.

4. CONCLUSIONS

In this paper, we have proposed a fuzzy detector-based adversarial attack detection method, a simple yet effective replacement to the conventional crisp set-based decision-making pipelines. Differing from these pipelines, the difference degrees between clean and attacked feature maps provide rich information to improve the proposed model’s ability to detect adversarial attacks. Our evaluation with different datasets and attacks has demonstrated the high effectiveness of the proposed method. The proposed fuzzy detector represents a significant step toward the realization of fuzzy rule-based adversarial attack detection algorithms and opens many future research directions that would further improve its accuracy and generalisation, which could eventually make adversarial attack detection easily designed for real-world applications. In the future, we will investigate the potential of assessing fuzzy rules using a new threshold-based fitness function with redefined support and confidence measures to further improve the detection accuracy.

Acknowledgment

Research supported by the UKRI Trustworthy Autonomous Systems Node in Security/EPSC Grant EP/V026763/1.

5. REFERENCES

- [1] J. Liu, A. Levine, C. P. Lau, R. Chellappa, and S. Feizi, “Segment and complete: defending object detectors against adversarial patch attacks with robust patch detection,” *IEEE Conference on Computer Vision and Pattern Recognition (CVPR)*, 2022.
- [2] F. Tramèr, A. Kurakin, N. Papernot, D. Boneh, and P. Mc-Daniel, “Ensemble adversarial training: attacks and defenses,” *International Conference on Learning Representations (ICLR)*, 2018.

- [3] G. Cohen, G. Sapiro, and R. Giryes, "Detecting adversarial samples using influence functions and nearest neighbors," *IEEE Conference on Computer Vision and Pattern Recognition (CVPR)*, 2020.
- [4] Y. Li, P. Angelov, and N. Suri, "Domain generalization and feature fusion for cross-domain imperceptible adversarial attack detection," *International Joint Conference on Neural Networks (IJCNN)*, 2023.
- [5] D. Meng and H. Chen, "MagNet: a two-pronged defense against adversarial examples," *ACM Conference on Computer and Communications Security (CCS)*, 2017.
- [6] F. Iglesias, J. Milosevic, and T. Zseby, "Fuzzy classification boundaries against adversarial network attacks," *Fuzzy Sets and Systems*, vol. 368, pp. 20–35, 2019.
- [7] P. P. K. Chan, J. Zheng, H. Liu, E. C. C. Tsang, and D. S. Yeung, "Robustness analysis of classical and fuzzy decision trees under adversarial evasion attack," *Applied Soft Computing*, vol. 107, p. 107311, 2021.
- [8] P. Qi, T. Jiang, L. Wang, X. Yuan, and Z. Li, "Detection tolerant black-box adversarial attack against automatic modulation classification with deep learning," *IEEE Transactions on Reliability*, vol. 71, no. 2, pp. 674–686, 2022.
- [9] J. Chen, T. Yu, C. Wu, H. Zheng, W. Zhao, L. Pang, and H. Li, "Adversarial attack detection based on example semantics and model activation features," *International Conference on Data Science and Information Technology (DSIT)*, 2022.
- [10] P. Angelov and X. Zhou, "Evolving fuzzy-rule-based classifiers from data streams," *IEEE Transactions on Fuzzy Systems*, vol. 16, no. 6, pp. 1462–1475, 2008.
- [11] J. C. Bezdek, "Pattern recognition with fuzzy objective function algorithms," *Springer Science Business Media*, 2013.
- [12] M. Hu, Y. Zhong, S. Xie, H. Lv, and Z. Lv, "Fuzzy system based medical image processing for brain disease prediction," *Frontiers in Neuroscience*, vol. 15, no. 714318, pp. 1–13, 2021.
- [13] J.-J. Liu and J.-C. Fan, "A novel fuzzy c-means clustering algorithm based on local density," *International Conference on Intelligent Information Processing (IIP)*, 2020.
- [14] T. J. Ross, "Fuzzy logic with engineering applications," *John Wiley Sons Ltd*, 2004.
- [15] E. Soares, P. Angelov, and N. Suri, "Similarity-based deep neural network to detect imperceptible adversarial attacks," *IEEE Symposium Series on Computational Intelligence (IEEE SSCI)*, 2022.
- [16] D. Hendrycks, S. Basart, N. Mu, S. Kadavath, F. Wang, E. Dorundo, R. Desai, T. Zhu, S. Parajuli, M. Guo, D. Song, J. Steinhardt, and J. Gilmer, "The many faces of robustness: a critical analysis of out-of-distribution generalization," *IEEE/CVF International Conference on Computer Vision (ICCV)*, 2021.
- [17] A. Krizhevsky, "Learning multiple layers of features from tiny images," *Master's thesis*, 2009.
- [18] T.-Y. Lin, M. Maire, S. Belongie, L. Bourdev, R. Girshick, J. Hays, P. Perona, D. Ramanan, C. L. Zitnick, and P. Dollár, "Microsoft COCO: common objects in context," *European Conference on Computer Vision (ECCV)*, 2014.
- [19] A. Howard, E. Park, and W. Kan, "Imagenet object localization challenge," *International Journal of Computer Vision (IJCV)*, 2015.
- [20] I. J. Goodfellow, J. Shlens, and C. Szegedy, "Explaining and harnessing adversarial examples," *International Conference on Learning Representations (ICLR)*, 2015.
- [21] A. Madry, A. Makelov, L. Schmidt, D. Tsipras, and A. Vladu, "Towards deep learning models resistant to adversarial attacks," *International Conference on Machine Learning (ICML)*, 2017.
- [22] C. Luo, Q. Lin, W. Xie, B. Wu, J. Xie, and L. Shen, "Frequency-driven imperceptible adversarial attack on semantic similarity," *IEEE Conference on Computer Vision and Pattern Recognition (CVPR)*, 2022.
- [23] M. Tan and Q. V. Le, "EfficientNetV2: smaller models and faster training," *International Conference on Machine Learning (ICML)*, 2021.
- [24] S.-H. Gao, M.-M. Cheng, K. Zhao, X.-Y. Zhang, M.-H. Yang, and P. Torr, "Res2Net: A New Multi-scale Backbone Architecture," *IEEE Transactions on Pattern Analysis and Machine Intelligence*, vol. 43, no. 2, pp. 652–662, 2021.
- [25] Z. Ge, S. Liu, F. Wang, Z. Li, and J. Sun, "YOLOX: exceeding YOLO series in 2021," *arXiv preprint arXiv:2107.08430*, 2021.
- [26] P.-Y. Chen, M.-C. Chang, J.-W. Hsieh, and Y.-S. Chen, "Parallel residual bi-fusion feature pyramid network for accurate single-shot object detection," *IEEE transactions on Image Processing*, vol. 30, pp. 9099–9111, 2021.